Mis-expression of the *CLV3/ESR*-like gene *CLE19* in *Arabidopsis* leads to a consumption of root meristem

Martijn Fiers[a], Gerd Hause[b], Kim Boutilier[a], Eva Casamitjana-Martinez[c],
Dolf Weijers[d], Remko Offringa[d], Lonneke van der Geest[a],
Michiel van Lookeren Campagne[a,1], Chun-Ming Liu[a,*]

[a] *Plant Research International, B.V., P.O. Box 16, 6700 AA Wageningen, The Netherlands*
[b] *Biocenter, University of Halle, D-06122 Halle, Germany*
[c] *Developmental Genetics, Utrecht University, Padualaan 8, 3584 CH Utrecht, The Netherlands*
[d] *Institute of Molecular Plant Sciences, Leiden University, Wassenaarseweg 64, Leiden, The Netherlands*

Abstract

Mild heat shock treatment (32 °C) of isolated *Brassica napus* microspores triggers a developmental switch from pollen maturation to embryo formation. This in vitro system was used to identify genes expressed in globular to heart-shape transition embryos. One of the genes isolated encodes a putative extra-cellular protein that exhibits high sequence similarity with the in silico identified *CLV3/ESR-related 19* polypeptide from *Arabidopsis* (*AtCLE19*) and was therefore named *BnCLE19*. *BnCLE19* is expressed in the primordia of cotyledons, sepals and cauline leaves, and in some pericycle cells in the root maturation zone. Mis-expression of *BnCLE19* or *AtCLE19* in *Arabidopsis* under the control of the CaMV 35S promoter resulted in a dramatic consumption of the root meristem, the formations of pin-shaped pistils and vascular islands. These results imply a role of *CLE19* in promoting cell differentiation or inhibiting cell division.
© 2003 Elsevier B.V. All rights reserved.

Keywords: CLE family; Embryogenesis; Cotyledon; Meristem; Differentiation

1. Introduction

Embryogenesis establishes the basic body plan for the adult plant, with the cotyledon(s), shoot apical meristem, hypocotyl and root meristem as the primary morphological domains along the apical-basal axis, and the epidermis, cortex and vascular bundles as the fundamental tissue structures along the radial axis (Jürgens et al., 1994). Several approaches have been used to identify genes involved in embryogenesis. Screening for *Arabidopsis*

mutants defective at either the embryo development or the seed germination stage has identified genes that are essential for embryo development (Jürgens et al., 1994; Liu and Meinke, 1998). Another gene identification method that has been widely used is differential gene expression analysis. Molecular analysis on early zygotic embryos is, however, complicated by the fact that zygotic embryos are very small and encased by a mass of endosperm and maternal tissues. Microspore-derived haploid embryos (Heck et al., 1995; Custers et al., 2001; Boutilier et al., 2002) provide efficient alternatives to obtain a large amount of relatively synchronized embryo material.

These studies have identified a number of genes involved in embryo development. The expression of some of these genes, such as *AGL15*, *BBM1* and *PEI1,* etc., lack apparent organ or tissue specificity but these genes appear to play general roles in embryo development (Heck et al., 1995; Li and Thomas, 1998; Boutilier et al., 2002). Other embryo regulatory genes are only expressed in certain cells of the

---

embryo, for example, the *WUS*, *CUC1*, *2 and 3*, *STM*, *UFO*, *CLV1* and *CLV3* in the shoot apical meristem (Vroemen et al., 2003; for review, see Sharma and Fletcher, 2002; Groß-Hardt and Laux, 2003) and the *PID* and *ANT* gene in the cotyledons (Long and Barton, 1998; Christensen et al., 2000). Functional analysis of these genes has greatly improved our understanding of discrete aspects of plant embryo development. Nevertheless, we are still far away from a complete picture of the complex molecular machinery behind this process.

In this report, we describe the use of the *Brassica napus* microspore embryogenesis system to identify genes expressed in embryos at the transition from the globular to heart-shape stage. One of the genes identified, named *BnCLE19*, is the orthologue of the in silico identified gene *AtCLE19* from *Arabidopsis* (Cock and McCormick, 2001). *AtCLE19* is a member of the *CLV3/ESR-related* (*CLE*) genes that encode small putative extra-cellular proteins with a conserved C-terminal box shared by the CLV3 peptide ligand (Fletcher et al., 1999; Cock and McCormick, 2001). Northern blotting showed that *BnCLE19* is expressed in globular to heart-shaped embryos and young pistils. Detailed expression analysis was performed in transgenic *Arabidopsis* plants carrying either a *BnCLE19* promoter∷ β-*glucuronidase A* (*GUS*) fusion construct or *GAL4-UAS* based transactivation constructs with a GFP-GUS fusion gene as a reporter, which showed that *BnCLE19* is expressed in certain differentiating cells such as primordia of cotyledons, sepals and cauline leaves, and in some pericycle cells in the root maturation zone. Mis-expression of *BnCLE19* or *AtCLE19* in *Arabidopsis* under the control of the *CaMV* 35S promoter resulted in the formations of pin-shaped pistils and vascular islands, and a dramatic consumption of the root meristem without affecting lateral root induction.

2. Materials and methods

2.1. Plant materials and microspore embryogenesis culture

Double-haploid *B. napus* L. cv. Topas DH4079 plants were maintained, and the isolation and culture of microspores were performed as previously described (Custers et al., 1994). *Arabidopsis thaliana* (ecotype C24 and Columbia) were grown in a greenhouse at 22 ± 3 °C, 15 hr. daylight.

2.2. Differential display reverse transcription PCR (DD-RT-PCR)

DD-RT-PCR was performed using the RNAmap Kit B (GeneHunter, Frederick, MD, USA) according to the manufacturer's recommendations. Total RNAs from freshly isolated microspores, non-embryogenic microspores cultured at 18 °C (8 hours), embryogenic microspores cultured at 32 °C (8 hours, 10 days, 16 days), and leaf tissue of *B. napus* were isolated as described by Ausubel et al. (1990) and DNase I treated using the MessageClean Kit (Gene-Hunter). Control material was obtained by heat shocking microspores at 41 °C, a condition that does not lead to embryogenesis (Custers et al., 1994). The expression pattern of differentially expressed DD-RT-PCR clones was confirmed using Northern blot analysis.

2.3. RNA gel blot analyses, cDNA isolation and RT-PCR

For RNA gel blot analysis in *B. napus*, 10 μg of total RNAs from various tissues were denatured with glyoxal prior to electrophoresis and blotted onto a Hybond-N$^+$ membrane, which was then hybridized overnight at 65 °C and washed twice for 30 minutes at 65 °C with 0.2xSSC and 0.5% (W/V) SDS. Equal loading was based on ethidium bromide staining.

For Northern blot analysis of transgenic *Arabidopsis*, total RNA was isolated from roots excised from 2-week old seedlings grown on 1/2MS salts with 1% sucrose and 1.5% agar. One microgram of total RNA was loaded on gel and blotted as described above and hybridised with radioactively labelled *BnCLE19* cDNA. Actin was used as a control.

For the isolation of the *BnCLE19* cDNA, an Uni-ZAP XR cDNA library (Stratagene) was constructed using poly(A)$^+$ RNA from globular to heart-shape *B. napus* microspore-derived embryos. Approximately 10^6 plaques were screened under high-stringency conditions with the cDNA fragment isolated from the DD-RT-PCR as a probe. The First Choice RLM-RACE Kit from Ambion (Cambridgeshire, UK) was used to amplify the full-length *AtCLE19* transcript from *Arabidopsis* inflorescence. The obtained cDNAs were cloned and sequenced.

For RT-PCR, cDNAs were prepared from total RNA of *Arabidopsis* isolated from cauline leaves, inflorescence, stems, roots, heart-shaped zygotic embryos, flower buds, petals and anthers using the RNeasy Plant Mini Kit (Qiagen, Valencia, USA), and then treated with DNase I (Invitrogen, Breda, NL). RT-PCR on actin (5′-GCGGTTTTCCCC-AGTGTTGTTG-3′; 5′-TGCCTGGACCTGCTTCATCA-TACT-3′) was used to quantify the cDNAs. Two primers (5′-TCCCCATCAAACAAACAAAAAC-3′; 5′-GATAC-ACATATAATTGTTCTTC-3′) located at 5′ and 3′ UTR of *CLE19* cDNA, were used to determine the expression pattern of *AtCLE19* in *Arabidopsis*. After optimisation, 35 and 41 cycles were used to amplify actin and *AtCLE19*, respectively.

2.4. Isolation of the BnCLE19 promoter and construction of GUS and GFP reporter construct

The Universal Genome Walker Kit (Clontech, Palo Alto, USA) was used to isolate genomic DNA fragments upstream of the *BnCLE19* coding region. The nested PCR was carried out using the adapter primer 1 supplied by the manufacturer

and *BnCLE19* specific primers: 5′-CCATTCTTCATCA-GCAAACTCCGAAATGA-3′ and 5′-CAGAAAAGAG-GAAGCCAATATCAAACTC-3′. A fusion construct (*pBnCLE19::GUS*) was made by the insertion of *BnCLE19* promoter (from 0 to 1086 bp, GenBank accession no. AF343658) into a vector that has an intron-containing GUS gene and a nopaline synthase terminator. The expression cassette was then excised and inserted into the binary vector pBINPLUS (van Engelen et al., 1995). The derived construct was confirmed by sequencing and transferred to *Agrobacterium tumefaciens* C58C1PMP90, and then transformed to *A. thaliana* ecotype C24 using the floral dip method (Clough and Bent, 1998).

The same promoter sequence was fused to an artificial transcription factor *GAL4-VP16* gene (*pBnCLE19::GAL4-VP16*) and delivered to *Arabidopsis* (Columbia) using the floral dip method. After homozygous lines were obtained, they were crossed to homozygous effector lines carrying a GFP-GUS fusion gene under the control of GAL4-VP16 binding sequence UAS (*pUAS::GFP-GUS*). This is the so-called transactivation system (Benjamins et al., 2001).

2.5. Ectopic expression of BnCLE19 and AtCLE19 in Arabidopsis

The full-length ORFs of *BnCLE19* and *AtCLE19* were cloned behind the double-enhanced *CaMV 35S* promoter (from -395 to -90 and from -525 to -1) and an AMV translational enhancer, as described by Datla et al. (1993). Transgenic plants of *Arabidopsis* (C24) were made and root development and geotropism were studied by growing the progeny seedlings on vertically cultured plates with the same medium mentioned above.

2.6. T-DNA insertion knockout of AtCLE19 in Arabidopsis

Three T-DNA insertion populations, the Wisconsin Knockout Center (http://www.biotech.wisc.edu/Arabidopsis/), the SAIL population at Syngenta (http://tmri.org/pages/collaborations/garlic_files/GarlicDescription.html) and the GABI-Kat in Germany (http://www.mpiz-koeln.mpg.de/GABI-Kat/), were searched either by PCR-based analysis or database mining to identify putative insertion lines. Insertions in the *AtCLE19* gene were confirmed by PCR analysis and sequencing. Homozygous progeny plants were identified through plating seeds from each progeny plant on selection media in combination with PCR analyses using primers for the T-DNA and the *AtCLE19* gene.

2.7. GUS assay, whole-mount clearing and cryo-electron microscopy

A modified GUS assay was carried out by following the method described by Jefferson et al. (1987) with 2 mM ferricyanide and ferrocyanide each in the reaction buffer. At least five independent transgenic lines were used for the GUS or GFP assay. To define the precise expression pattern of *BnCLE19* during embryogenesis, zygotic embryos from transgenic plants were excised from seed and then stained for GUS activity. For the whole-mount clearing and observation of root and flower, samples were prepared as described by Sabatini et al. (1999). Dark-field microscopy was used to observe the vascular pattern in cleared flower samples. For detailed observation, GUS stained materials were fixed and embedded in paraffin and sectioned to 7 μm before observed under a Nomarski microscope. For cryo-electron microscopy, plant materials were glued to copper stubs using conductive carbon glue and freeze immediately in liquid nitrogen. The samples were then transferred to a low temperature field emission scanning electron microscope (LT-FESEM, JSM 6300F, JEOL, Japan) equipped with an Oxford cryo-chamber. After a light coating with argon gas the samples were observed and pictures were taken with a digital camera.

For confocal analysis of *BnCLE19* promoter activity in *Arabidopsis*, F1 embryos carrying both transactivation constructs (*pBnCLE19::GAL4-VP16* and *pUAS::GFP-GUS*) were excised from ovules at different developmental stages, and transferred directly to a glass slide with 5% glycerol solution, and observed under a confocal microscope.

3. Results

3.1. Isolation of differentially expressed genes from B. napus microspore-derived embryos

Mild heat shock treatment (32 °C) of isolated *B. napus* microspores triggers a developmental switch from pollen maturation to embryo formation, while culturing at 18 °C leads to pollen maturation (Fig. 1A). Embryo samples at the globular to heart-shaped transition stage (10 days after culture) were analyzed using DD-RT-PCR for genes that are either up- or down-regulated during this developmental change. Embryos at this stage change from a relatively unorganised globe to a 'mini-plant' with bilateral symmetry, in which the major tissue and organ primordia are established. Torpedo staged embryos (16 days after culture), leaf material and microspores treated at 18 or 41 °C (a condition that does not trigger embryogenesis) were used as controls. Genes showing developmentally regulated expression profiles were studied further (Custers et al., 2001). Here we present the characterization of one of these genes named *BnCLE19* (originally named *LLP1*), which is up-regulated in embryos at the globular stage and onwards (Fig. 1B, indicated by an arrow).

3.2. cDNA isolation

The *BnCLE19* DD-RT-PCR fragment was used to obtain a full-length transcript from a cDNA library prepared from
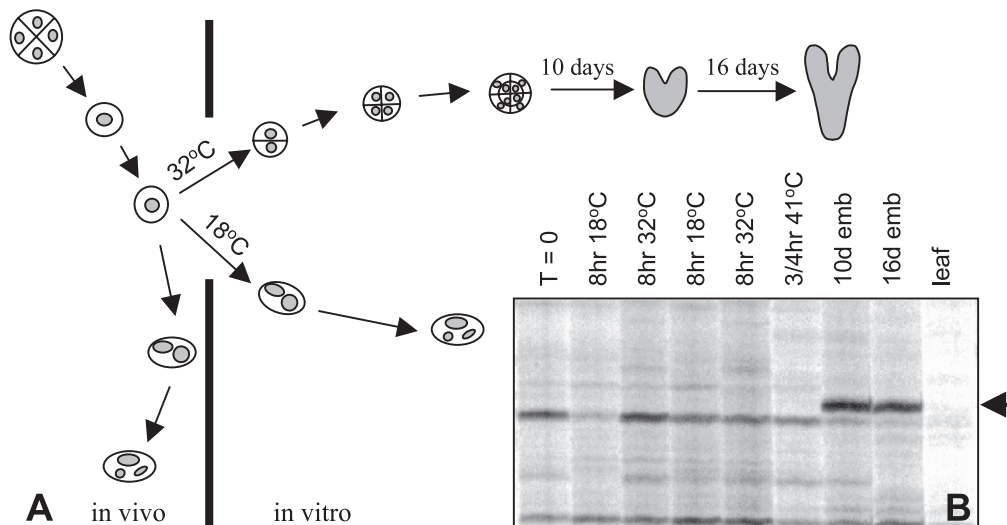
Fig. 1. Isolation of *BnCLE19* from microspore-derived embryos of *B. napus* by DD-RT-PCR. (A) Schematic presentation of the *B. napus* microspore culture system used to obtain a large amount of relatively synchronised embryos. Immature microspores at the late uni-cellular and early bi-cellular stages were isolated and cultured at different temperatures, leading to either embryogenesis (32 °C) or pollen maturation (18 °C). (B) A portion of the DD-RT-PCR auto-radiograph showing the expression of *BnCLE19* (arrow) in *B. napus* embryos after 10 days (globular to heart-shaped stage) and 16 days (torpedo stage) of culture at 32 °C. *BnCLE19* mRNA was not detectable in freshly isolated microspores (*T* = 0), in microspores cultured for 8 h at 18 or 32 °C, or at 41 °C for 45 min, or in leaves.

10-day old microspore embryo cultures. A 417 bp cDNA clone encoding a 74-aa putative extra-cellular peptide was identified (Fig. 2A). Two stop codons located upstream of the longest open reading frame (ORF), suggested that a full-length ORF was obtained (GenBank accession no. AF343656). Queries with the *BnCLE19* sequence to the *Arabidopsis* genome revealed similarity to *AtCLE19*, which was identified in silico through database mining (Fig. 2B;

Fig. 2. *BnCLE19* encodes a CLV3-like extra-cellular protein. (A) The *BnCLE19* cDNA was isolated from a cDNA library prepared from globular to heart-shape embryos obtained from *B. napus* microspore culture. The Two stop codons before the longest ORF are marked with triple asterisks (***). The DD-RT-PCR fragment (underlined) represents a partial *BnCLE19* cDNA sequence. The signal peptide is shown in bold. An asterisk indicates the functional stop codon. (B) Alignment of *BnCLE19* with *CLE19*, *CLE21*, *CLV3*, *ZmESR3*, *CLE26*, and *HgCLE*. The conserved identical amino acids are shaded in black, and similar amino acids in grey. The putative signal peptide cleavage site for *BnCLE19* and *CLE19* is marked with an arrowhead and the conserved CLE box is framed.

Cock and McCormick, 2001). However, isolation of full-length capped cDNAs from *Arabidopsis* showed that the transcription start site of *AtCLE19* (GenBank accession no. AF343657) begins 72 bp after the previously predicted translational start codon (ATG), resulting in a polypeptide with the same length as the *BnCLE19*, but 58 amino acids shorter than the previously annotated *AtCLE19* (Cock and McCormick, 2001). The new annotation of *AtCLE19* led to an increased probability that the predicted protein contains a signal peptide (from 37.5% to 99.8%, Fig. 2A, in bold). Neither *BnCLE19* nor *AtCLE19* contain introns. Within the 225 bp coding region, they share 83% and 68% sequence identity at the DNA and protein levels, respectively. Therefore, *AtCLE19* in *Arabidopsis* should be the orthologue of *BnCLE19* in *B. napus*.

CLE19 is a member of the *CLV3/ESR-related* (*CLE*) family of genes that encode polypeptides with several common features. All of the *CLE* genes encode small proteins (average Mr 7.7 kDa), that have an N-terminal putative signal peptide or a membrane anchor, and contain a conserved 14-AA motif (KRXVPXGPNPLHNR) located at or near their C-termini (Fig. 2B, termed CLE box accordingly; Cock and McCormick, 2001; Sharma et al., 2003). There are 26 *CLE* members in *Arabidopsis* genome (Cock and McCormick, 2001; Sharma et al., 2003). RT-PCR has shown that all of them except one (*CLE26*) are expressed in one or more tissues during development (Sharma et al., 2003). Some CLEs, such as *CLV3*, ZmESR3, CLE26 and HgCLE, have a 10- to 53-amino acid extension after the CLE box (Fig. 2B; Cock and McCormick, 2001). *CLV3* is an extra-cellular peptide ligand and is expressed in the putative stem cells of shoot and floral meristems, and functions in restricting the number of stem cells through its interaction with the CLV1/CLV2 receptor complex and the WUS transcription factor (Fletcher et al., 1999; Schoof et al., 2000; Brand et al., 2000). *ZmESR3* encodes a secreted protein and is expressed in a small region of endosperm surrounding the maize embryo (Opsahl-Ferstad et al., 1997). Recently, a CLE protein (HgCLE, Fig. 2B) has also been identified in a soybean cyst nematode, suggesting that the parasitic nematode may have co-opted the plant signalling peptide to enable interaction with the host cells (Olsen and Skriver, 2003).

No matching *AtCLE19* cDNA was found among 113,330 ESTs available in the *Arabidopsis* database. An explanation could be that most cDNA libraries are constructed using size-fractionated cDNA. Genes such as *AtCLE19* with short transcripts may only be present in very low abundance in these libraries.

3.3. The expression of BnCLE19

Northern blot analysis of RNA from *B. napus* tissues demonstrated relatively high levels of *BnCLE19* expression in globular to heart shape embryos and in young flower buds (1–4 mm in length). In 5 mm long flower buds, the expression was only detected in pistils (Fig. 3A).

To determine the detailed spatial pattern of *BnCLE19* expression, a 1086 bp genomic sequence (GenBank accession no. AF343658) upstream of the *BnCLE19* ORF was
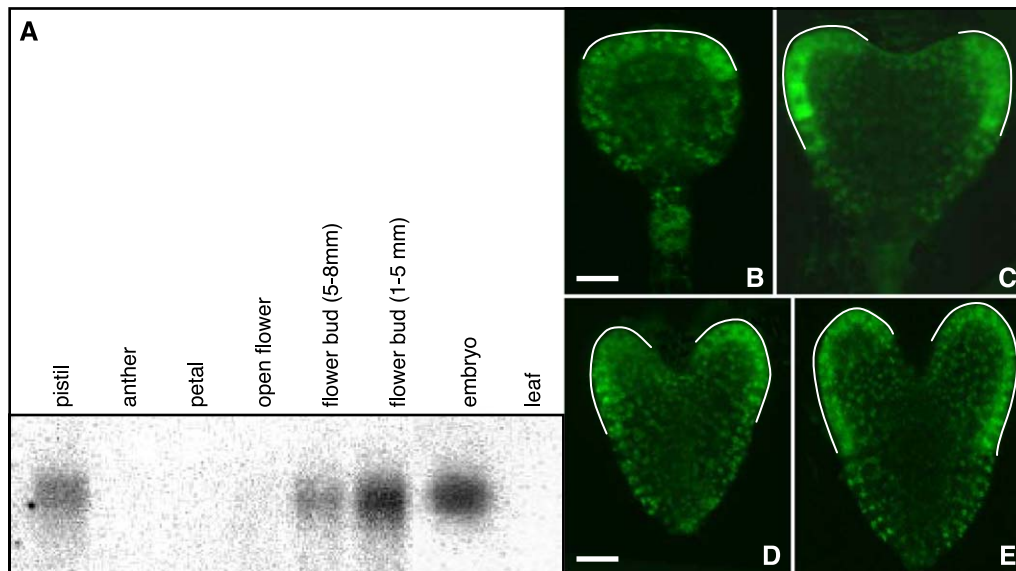

Fig. 3. Expression analysis of *BnCLE19*. (A) Northern blot analysis of *BnCLE19* expression in *B. napus*. Ten micrograms of total RNA isolated from various organs and tissues was separated, blotted and probed with the *BnCLE19* cDNA. *BnCLE19* is expressed in developing embryos (globular to heart stage embryos from microspore culture), flower buds and pistils. Petals, anthers and pistils were obtained from 5 mm flower buds containing tri-nucleate pollen. (B–E) Expression of *BnCLE19* in zygotic embryos, as shown by the confocal microscopic observation of F1 embryos carrying both *pBnCLE19::GAL4-VP16*) and *pUAS::GFP-GUS* constructs. In tri-angular stage embryos, GFP expression was observed in the epidermal cell layer that covers the cotyledon primordia and the shoot apical meristem (B). In the heart-to-torpedo-shaped embryos, the GFP signal was only observed in the epidermal cells covering the cotyledon primordia (C–E). The scale bars in (B) represents 10 μm for (B and C), and in (D) represents 25 μm for (D and E).

isolated from *B. napus* and fused to the *GAL4-VP16* transcription factor gene (*pBnCLE19*::*GAL4-VP16*) that consequently drove the expression of the *pUAS*::GFP-GUS fusion construct after crossing homozygous lines carrying these individual constructs. F1 embryos were analysed for GFP pattern under a confocal microscope to determine the *BnCLE19* promoter activity during embryogenesis. As showed in Fig. 3B–E, GFP expression was first detected in tri-angular embryos, in a single layer of protoderm cells covering the cotyledon primordia and the shoot apical meristem (Fig. 3B, indicated by a curved line along the cells). From the heart-shape to the early torpedo stage, GFP was only expressed in the epidermal cells covering the

newly formed cotyledons, but not in those ones along the shoot apical meristem (Fig. 3C–E). At the bent-cotyledon stage the expression was shifted to the basal region of the cotyledons and switched off completely in cotyledon staged embryos (data not shown).

The same promoter sequence was fused to *GUS* reporter gene (producing construct *pBnCLE19*::*GUS*), and transformed to *Arabidopsis* (Jefferson et al., 1987) to define the *BnCLE19* promoter activity in a whole plant level. After seed germination, the first detectable GUS expression was seen in a tissue layer in and slightly above the root hair region, after the main root was longer than 1 cm (Fig. 4A–D). GUS staining was not observed in the roots with
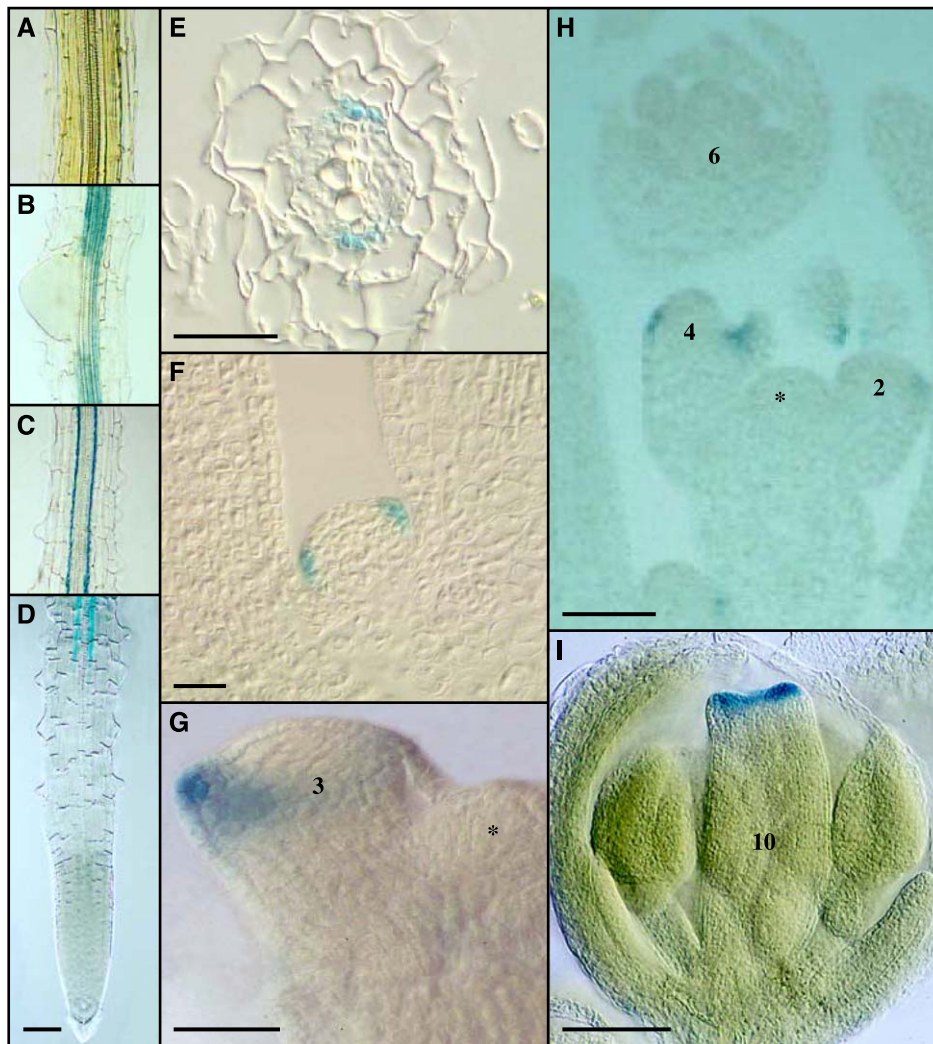

Fig. 4. Histological analysis of post-embryonic *GUS* expression in *pBnCLE19-GUS* transgenic *Arabidopsis*. The photographs correspond to whole-mount materials cleared with Hoyer's solution (A–C, F and H) and paraffin sections (D, E and G). (A–D) In roots, *pBnCLE19*::*GUS* is expressed in the root hair region and the differentiation zone above (B–D), but not in the root meristem (D), nor in the newly formed lateral root (B), nor in older roots with secondary thickenings (A). The scale bar in (D) represents 100 μm for A–D. (E) Transverse section of a root in the root hair region, showing GUS expression in two to three pericycle cells facing the protoxylem poles. The tissue deformation was caused by the acetone pre-fixation used in the GUS assay. The scale bar represents 100 μm. (F) *pBnCLE19*::*GUS* expression was seen in the periphery of meristems in the axillary bud, where the cauline leaves will form. The scale bar represents 25 μm (G and H). During flower development, GUS expression was seen in the sepal primordia in stage two to five flower buds, but not in the main inflorescence meristem (marked with an asterisk). The scale bars represent 40 μm. (I) In a stage 10 flower bud, GUS expression was seen at the top of the pistil, where the stigma hairs will form. The scale bar represents 150 μm.

secondary thickening, nor in the root meristem (Fig. 4A and D), hypocotyl and cotyledons (data not shown). In radial sections, *GUS* expression was observed in a few pericycle cells facing the protoxylem poles (Fig. 4C and E). The expression in lateral roots was comparable to that in the main root and could only be observed after root hairs emerged (data not shown).

In above ground tissues, the first detectable *GUS* expression was seen in the periphery of the axillary meristems (Fig. 4F). In expanding leaves faint *GUS* expression was observed in the abaxial side of the petioles (data not shown), which vanished in fully expanded leaves (data not shown). No *GUS* expression was observed in the central domain of the meristem (Fig. 4F–H). During floral development, *GUS* was expressed in the sepal primordia during floral stages 2–5 (Fig. 4G and H; see Smyth et al., 1990 for the floral stage definitions). *GUS* expression was restricted to the stigma in flower buds between stage 7 and stage 10 (Fig. 4I), and switched off completely shortly before the flower opened.

Among 6 *pBnCLE19::GUS* and 5 F1 transactivation lines tested, the expression pattern was consistent among different lines although the intensity varied slightly.

3.4. AtCLE19 is expressed in a similar manner as BnCLE19

A conserved regulatory function for the *AtCLE19* and *BnCLE19* promoters is expected based on the nucleotide similarity between these two promoters. *BnCLE19* and *AtCLE19* exhibit 81% sequence similarity in a 415 bp region upstream of the start codon, and a TATA box (TATAAA) was identified for both genes at 128 bp before the start of the ORF. We used RT-PCR to determine the expression pattern of *AtCLE19*. The results showed that, *AtCLE19* in *Arabidopsis* is strongly expressed in heart-shape embryos and young flower buds, weakly expressed in inflorescence, faintly expressed in leaves and roots (visible on gel only when 5 times more cDNA was used, data not shown), and is not detectable in stems, petals and anthers (Fig. 5). This expression pattern is consistent with the expression pattern of *BnCLE19*, but not the same as reported by Sharma et al. (2003), who have showed that *AtCLE19* is also expressed in pollen.

3.5. Ectopic mis-expression of BnCLE19 and AtCLE19 in Arabidopsis under the control of CaMV 35S promoter

A double enhanced CaMV 35S promoter with an AMV translational enhancer (Datla et al., 1993) was used to drive the expression of the *BnCLE19* (and *AtCLE19* cDNA (*p35S::AtCLE19*) in *Arabidopsis* (C24). Thirteen out of 75 *p35S::BnCLE19* transformants and 2 out of 24 *p35S::BnCLE19* transformants exhibited short roots, slow growth, late flowering and pin-shaped pistil phenotypes. Many other lines showed short root phenotype but without pin-shaped pistils. The frequency of flowers with pin-shaped pistils varies from 5% to 50% in different trans-
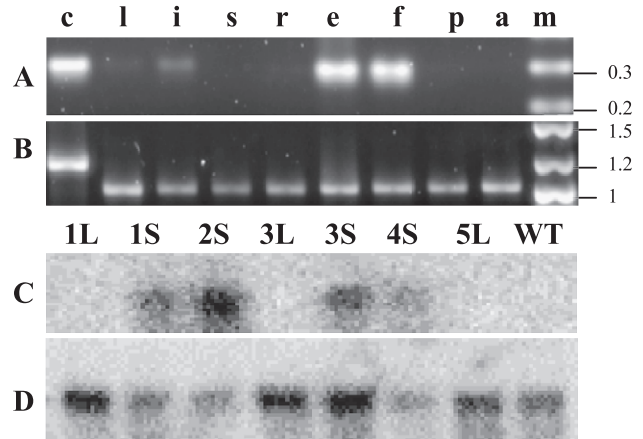

Fig. 5. Expression analysis. (A–B) *AtCLE19* is expressed in a similar manner as *BnCLE19*, as shown by RT-PCR analysis (top panel). *AtCLE19* (A) is strongly expressed in heart-shape embryos (e) and flower buds (f), intermediate in inflorescence (i) and weakly expressed in leaves (l) and roots (r) (leaves and roots only visible when 5 times more cDNA was used), and not detectable in stems (s), petal (p) and anther (a). c: chromosomal DNA, m: molecular weight marker. Actin was used as a control (B). The numbers at the side denote the molecular size in kb. (C–D) Expression of *BnCLE19* (C) and actin (D) in the roots excised from T2 transgenic and non-transgenic *Arabidopsis* seedlings (C24). One microgram of total RNAs was used for the Northern blot analysis. 1L: seedlings with long roots segregated from transgenic line #1; 1S: seedlings with short roots from line #1; 2S: seedlings with short roots from line #2; 3L: wildtype-looking seedlings (long roots) segregated from transgenic line #3; 3S: seedlings from line #3, with short roots and pin-shaped pistils; 4S: seedlings from line #4 with short roots; 5L: seedlings from transgenic line #5, with long roots. WT: wildtype C24 seedlings. Note that elevated expression of *BnCLE19* in transgenic *Arabidopsis* roots correlates with the short root phenotype. Lines #3 and #4 showed pin-shaped pistils in flowers but lines #1 and #2 did not.

genic lines, which is relatively consistent though generations. Bolting did not occur until 40–45 days after seeds were planted, instead of after 20 days in the wildtype. In contrast to one paraclade normally produced from each axillary bud in wildtypes, multiple ones (up to 7) were often formed sequentially in the mis-expression lines, particularly in the axils of cauline leaves. No embryo lethals were observed in these lines. Genetic analysis indicated that their phenotypes were inherited as a dominant trait in Mendelian fashion and linked with the transgene (Fig. 6A). The phenotype persists through generations (four generations tested).

Northern blot analysis of five transgenic lines carrying the *BnCLE19* construct showed that the short root phenotype is linked to the elevated expression of *BnCLE19* gene in the roots. As showed in Fig. 5C, all seedlings with a short root phenotype (1S, 2S, 3S and 4S) showed high level of expression of BnCLE19. Neither the wildtype (lane WT), nor the transgenic plants without any phenotype (lane 5L), or the normal long root plants (lanes 1L and 3L) segregated from hemizygous parental plants gave detectable expression when 1 μg of root total RNA was analyzed on gel (Fig. 5C and D). As compared to those lines with only short root phenotypes (lines #1 and #2), lines exhibited both the short root and the
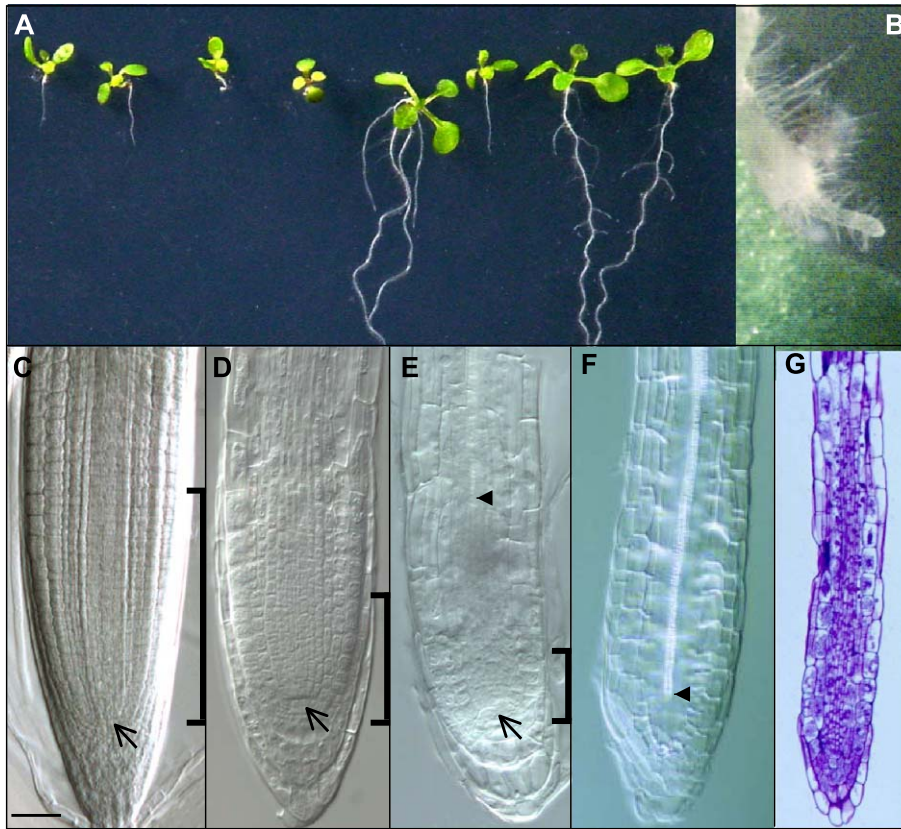
Fig. 6. Ectopic expression of *BnCLE19* in *Arabidopsis* led to a consumption of root meristems. The root meristems are marked with a square bracket in C to E, and the QC cells are marked with an arrow. (A) Two-week old progeny seedlings from a hemizygous *p35S::BnCLE19* parental plant were growing on a vertically culture plate, showing segregation for transgenic seedlings with a dominant short root phenotype and three seedlings being wildtype. Note that root geotropism was not affected in these short root seedlings. (B) A close-up observation of a *p35S::BnCLE19* root with the short root phenotype, showing the formation of root hairs to the root tip. (C) A whole-mount, 7-day old wildtype root of *Arabidopsis* observed under Nomarski optics. Note the gradual cell size changes from the root meristem to the elongation zone. No obvious pattern change occurred in the following week in the wildtype. (D) A primary root from a 7-day old *p35S::BnCLE19 Arabidopsis* line showing the reduced length of the root meristem. Note the evident cell size increase above the short meristem. (E) A primary root from a 10-day old *p35S::BnCLE19 Arabidopsis* line. Note the greatly reduced root meristem and the highly vacuolated cells above the meristem and the xylem elements (indicated by an arrowhead). The QC was still recognisable at this stage. (F) A primary root from a 2-week old *p35S::BnCLE19* seedling showing that the root eristem has disappeared completely. Note that the xylem elements (indicated by an arrowhead) reached the central cell zone. No QC can be found at this stage. (G) Longitudinal section of a root from a 10-day old *p35S::BnCLE19* seedling, showing the enlarged and

pin-shaped pistil phenotypes (lines #3 and #4) seems do not have higher expression of *BnCLE19* in roots (Fig. 5C).

Root geotropism (Fig. 6A) and lateral root initiation did not seem affected by mis-expression of *BnCLE19* and *AtCLE19* genes. Root hairs were formed almost to the tip of the roots (Fig. 6B). Tissue clearing, followed by Nomarski microscopy of the roots from *p35S::BnCLE19* transgenic plants showed that root meristematic tissue was gradually consumed during root growth and development (Fig. 6C–G). As compared to the wildtype (Fig. 6C), in *BnCLE19* mis-expression plants the root meristem zone became shorter, and was followed immediately by the formation of highly vacuolated cells that were typically seen in the root hair region (Figs. 6D, 7 days after plating). At this stage the quiescent center (QC) was still recognizable (indicated by an arrow). Ten days after germination, only a small number of meristematic cells were present in the root tip, but the QC was still visible (Fig. 6E). Tissue

sections of roots at this stage and staining with toluidine blue revealed the existence of well differentiated cells in the meristem region (Fig. 6G). Both the root meristematic cells and the QC disappeared in 2-week old *p35S::BnCLE19* seedlings (Fig. 6F). All the cells in this region became highly vacuolated and exhibited a thickening of their cell walls. Staining of starch showed that the columella identity was present even after the root meristem was fully differentiated (data not shown). Xylem elements reached the central cell region (Fig. 6F, indicated by an arrowhead). The expression of *BnCLE19* under the control of the *35S* promoter appears to have no influence on embryonic root formation and lateral root induction. The same phenotype was observed in the transgenic plants carrying the *p35S::AtCLE19* construct (data not shown), and when *AtCLE19* was expressed in *Arabidopsis* under the control of a root meristem-specific promoter, *RCH1* (Casamitjana-Martinez et al., 2003).
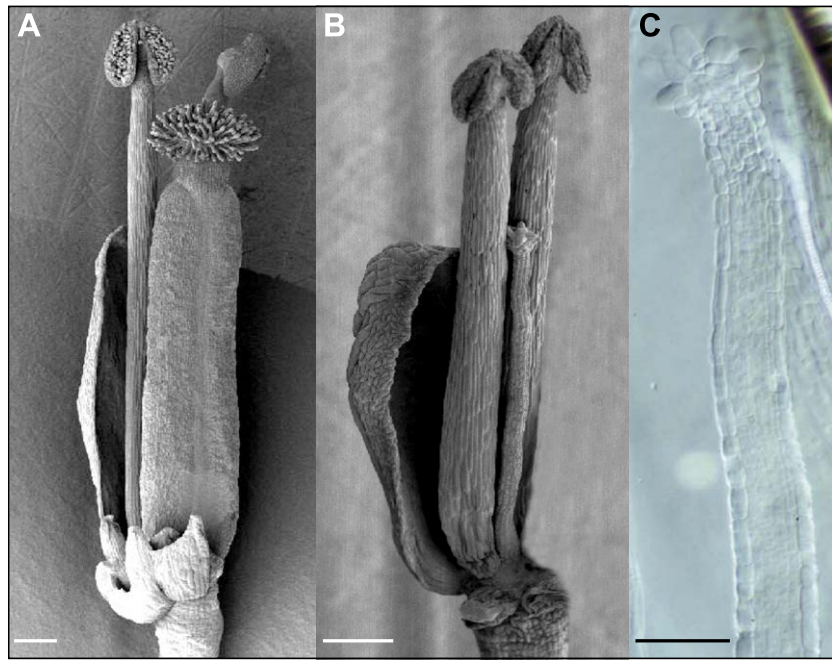
Fig. 7. The formation of pin-shaped pistils in *Arabidopsis* mis-expressing *BnCLE19*. (A) and (B) are photos from cryo-electron microscopy. (A) A wildtype open flower with some outer whorls removed to show the well-developed pistil. (B) An open flower from *p35S::BnCLE19* plants treated in the same way as in (A) to show the pin-shaped pistil. (C) Whole-mount clearing of an open flower from *p35S::BnCLE19* plant showing the pin-shaped pistil. Neither ovules, nor xylem were observed in such pistils. Note the stigma formed at the top of the pistil. The scale bars represent 200 μm for (A) and (B), 100 μm for (C).

The pin-shaped pistils observed in *BnCLE19* and *AtCLE19* misexpression plants have a filamentary structure that did not contain carpels and ovules (Fig. 7). In wild-type plants ca. 150 bulbous cells formed at the top of the stigma (Fig. 7A; Sessions and Zambryski, 1995), whereas only 18–20 such cells could be observed on the pin-shaped pistil (Fig. 7B and C). The region below the stigma, most likely corresponding to the style, had six-cell layers across the median section, which is much narrower than wild-type styles that have more than 30 cell layers. No vascular bundle was observed within these pin-shaped pistils. These pistils are quite different from those of *ettin* mutants in which the ovary is reduced but the style is expanded longitudinally. Occasionally, flowers without pistils were also observed in some transgenic lines. This phenotype could be the consequence of a consumption of floral meristem in whorl 4.

Furthermore, defective vascular development was observed in flowers of *BnCLE19* and *AtCLE19* mis-expression lines. In the wildtype inflorescence, vascular bundles are formed at stage 9 by extension from the main stem up to pedicels and then to floral organs (Fig. 8A). Xylem elements in the flower buds are established first in sepals and followed sequentially by pistils, stamens and petals, resulting in a complete vascular network (Fig. 8C). In *p35S::BnCLE19* flower buds, regional vascular formation without connecting to the main stems was often observed (Fig. 8D, indicated by arrowheads). These xylem elements ended at the receptacle region of the flower. The vascular connection failure seems to be associated with the forma-

tion of pin-shaped pistils, since this phenomenon was not observed in flowers with normal pistils. However, local xylem formation in sepals and petals, as vascular islands, was observed in normal flowers and flowers with a pin-shaped pistil (Fig. 8D, indicated by arrows). The same results were observed in *p35S::AtCLE19* transgenic plants (data not shown).

Since vascular differentiation is known to be associated with auxin flux (Aloni, 1987), we examined if the formation of vascular islands was caused by local accumulation of auxin. As shown previously, the *DR5::GUS* reporter construct can be used to monitor auxin distribution (Sabatini et al., 1999). In wild-type *Arabidopsis* roots, the highest GUS staining is observed in the QC cells of the root meristem (Sabatini et al., 1999). In the upper part of the plant, we observed that GUS staining was mainly in the anthers (Fig. 8B), in particular, the pollen grains after the uni-nucleate stage. We crossed the *DR5::GUS* line with the *p35S::BnCLE19* lines, and analyzed the progeny plants for *DR5::GUS* expression. In roots we observed that the high level of GUS staining in the QC cells persists right before the meristematic cells disappeared (data not shown), which is the same as the expression of *AtCLE19* under the control of *RCH1* promoter (Casamitjana-Martinez et al., 2003). In the flowers the same GUS pattern was also observed, regardless of whether the flower had a normal or pin-shaped pistil. This suggested that either *BnCLE19* functions downstream of the auxin signaling or that it acts through an auxin-independent pathway for promoting vascular development.
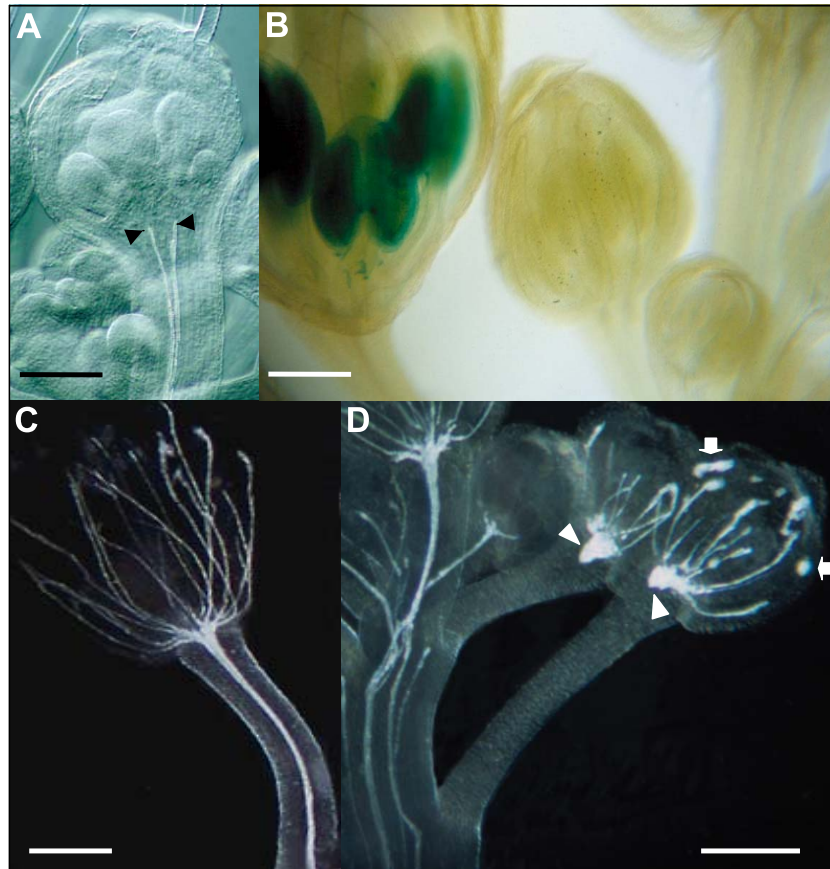
Fig. 8. Mis-expression of *BnCLE19* in *Arabidopsis* leads to a failure of xylem connections in flower buds. (A) Nomarski observation of a whole mount stage 9 wild-type flower bud from the wildtype, showing the extension of xylem elements (indicated by arrowheads) from the main stem towards the flower bud. (B) GUS staining of flower buds from a hybrid plant obtained from a cross between homozygous *DR5*::*GUS* and *p35S*::*BnCLE19* lines. The GUS staining was seen only in the anthers with uni-cellular microspores, which is the same as that in the *DR5*::*GUS* parental line. (C) Dark-field observation showing the well-developed xylem network in a wild-type flower bud. (D) Dark-field observation showing that mis-expression of *BnCLE19* leads to the formation of disconnected xylem elements in flower buds (indicated by arrowheads). Note also the vascular islands formed (indicated by arrows) in these flower buds. The scale bars represent 100 μm for (A), 150 μm for (B) and 400 μm in (C) and (D).

3.6. T-DNA insertion knockout of AtCLE19

To further analyze the function of the *CLE19* genes, T-DNA knockout lines were identified in different *Arabidopsis* insertion populations. In total three T-DNA insertions were obtained in the *AtCLE19* locus, with the insertion sites located at −218 bp (Wisconsin line), −40 bp (GABI-Kat line) and +130 bp (SAIL line, these numbers are in relation to the ATG of *AtCLE19*). Homozygous insertion lines were obtained from each transgenic line, however no visible phenotypes were observed as compared to the sibling heterozygous plants. The reasons for a lack of phenotype could either be that *AtCLE19* plays a minor role in plant development or that other *CLE* genes function redundantly with *CLE19*. Given the strong phenotypes observed in plants mis-expressing *BnCLE19* gene under the control of *35S* promoter and root-specific expression of *AtCLE19* under the *RCH1* promoter (Casamitjana-Martinez et al., 2003) in *Arabidopsis*, the first possibility is unlikely. With respect to the redundancy of AtCLE19, AtCLE21 shows the highest overall similarity with AtCLE19. These two poly-peptides exhibited 36.5% overall sequence identity, with only one amino acid difference in the CLE box. It is possible that *AtCLE21* may complement the *AtCLE19* function in the insertion lines.

4. Discussion

In the present research, we are interested in identifying genes expressed in embryos during the transition from globular to heart-shape stage of development. This is the period during which the embryo changes from a relatively unorganised globe to a 'mini-plant' with bilateral symmetry in which the major tissue and organ primordia are established. *BnCLE19* gene was isolated from *B. napus* microspore-derived embryos using the DD-RT-PCR technique. It encodes a putative extra-cellular protein with sequence similarity to the CLE19 polypeptide from *Arabidopsis* (Cock and McCormick, 2001). The *CLE* family consists of 26 genes in the *Arabidopsis* genome (Cock and McCormick, 2001; Sharma et al.,

2003). All of them except one (*CLE26*) are expressed in diverse tissues of *Arabidopsis* (Sharma et al., 2003). The encoded CLE polypeptides are characterized by their small sizes, an N-terminal secretion signal and a conserved C-terminal CLE motif shared by CLV3 and ZmESR3 (Cock and McCormick, 2001). *CLV3*, expressed in the stem cells of the shoot apical meristem, encodes an inter-cellular peptide ligand that acts through the CLV1/2 receptor complex to impose a negative signal to the stem cells, in balance with the stem cell-promoting signal generated by the WUS transcription factor expressed in the underlying organizing center (Fletcher et al., 1999; Brand et al., 2000; Schoof et al., 2000; Rojo et al., 2002; Lenhard and Laux, 2003). The balance between *CLV3* and WUS signals permits the onset of cell differentiation in the periphery and, at the same time, maintains a stable number of stem cells in the center of the shoot meristem (Lenhard and Laux, 2003). *ZmESR3* of maize is expressed in a small region of endosperm surrounding the embryo, but its function is not clear yet (Opsahl-Ferstad et al., 1997). CLE40 can functionally complement CLV3 when expressed under the control of CLV3 promoter (Hobe et al., 2003).

During embryogenesis, the expression of *BnCLE19* is associated with cotyledon development, which was first seen at the top of the late globular embryos prior to cotyledon initiation, at about the same time as the *PINOID* gene (Christensen et al., 2000). At the heart-shape and early torpedo stage, *BnCLE19* expression is restricted to the cotyledon primordia. Later the expression is narrowed down to the edge of the cotyledons and switched off completely in mature embryos. The expression pattern contrasts with *CLV3*, which is expressed in the shoot apical meristem (Fletcher et al., 1999) and several other cotyledon-expressed genes, such as *FIL* (Siegfried et al., 1999), *ANT* (Long and Barton, 1998), *PID* (Christensen et al., 2000) and *REV* (Otsuga et al., 2001). Like all known embryo development-related genes, *BnCLE19* was also expressed in post-embryo development. After seed germination, *BnCLE19* is expressed in the periphery of the axillary meristem, in sepal primordia, young stigma and in some pericycle cells at the root hair region. The common feature among these cells is the intermediate state of differentiation, which implies a role of *BnCLE19* in organogenesis or cell differentiation.

Mis-expression of *BnCLE19* and *AtCLE19* in *Arabidopsis* leads to a premature cell differentiation in several tissues. Firstly, *p35S::BnCLE19* and *p35S::AtCLE19* plants exhibited a short root phenotype, in which the primary root meristem was fully differentiated in 12-day-old seedlings. Root hairs were formed to the tip of the roots. The QC cells disappeared at about the same time when the meristem was fully differentiated, suggesting that the consumption of meristem may not be caused by the differentiation of QC. This is a phenotype shared by *CLE40* and *CLV3* mis-expressions (Hobe et al., 2003).

Secondly, pin-shaped pistils (pistil without carpel and ovule) were formed in plants mis-expressing *BnCLE19* and *AtCLE19*, which could be the consequence of a premature consumption of meristematic cells in the whorl 4 of these flowers. This phenotype is the opposite of the *clv3* mutant phenotype in which an increased number of carpels were observed. The third, flowers with disconnected vascular bundles were observed in *p35S::BnCLE19* and *p35S::AtCLE19* plants, which could be a premature differentiation of the xylem. As such, we hypothesize that, as a differentiation signal, the CLE19 polypeptide may be perceived by a receptor kinase complex in roots and floral organs, which then triggers pre-mature cell differentiation. Such a receptor complex may not be available in many meristematic cells, for example, the initiation phase of the root meristem since both embryonic root formation and the lateral root induction were not affected by the transgene. Based on the current evidence we cannot exclude a second possibility that the primary function of *CLE19* is to inhibit cell division rather than to promote cell differentiation or organogenesis.

Although the mis-expression of *CLE19* led to a strong phenotype in root and flower development in *Arabidopsis*, T-DNA insertions in the coding and the 5′ UTR regions showed no phenotype. This implies that either *CLE19* plays a minor role in normal development, or additional genes such as *CLE21* that has the highest sequence similarity with *CLE19* can complement the *CLE19* mutation.

Using the short root phenotype generated by mis-expression of *BnCLE19*, Casamitjana-Martinez et al. (2003) carried out a mutant screen for repressors of the root meristems consumption phenotype. A root meristem-specific promoter *pRCH1* was used to drive the expression of *CLE19* and a phenotype identical to that seen in *p35S::BnCLE19* roots was observed in the transgenic lines. Two genetic loci, *SOL* (*SUPPRESSOR OF RCH1-LLP1*) *1* and *SOL2*, were identified. It is interesting to note that the *sol2* mutant, similar to *clavata*, also exhibits an increased number of carpels which is the opposite to the pin-shaped pistil phenotype, suggesting that *SOL2* might be involved in the CLV signaling pathway to restrict the meristem size. The *SOL1* gene was cloned by chromosome walking, and found to encode a putative Zn^{2+}-carboxypeptidase. Casamitjana-Martinez et al. (2003) proposed that the CLE19 polypeptide may be further processed to produce a functional peptide ligand. If further processing of BnCLE19 does indeed occur, then it would also explain why our immunological studies of BnCLE19 using polyclonal antiserum have failed to detect any BnCLE19 signal in the inflorescence of cauliflower and *B. napus* (data not shown). The same may apply to the CLV3 ligand, since to date no one has been able to reproducibly detect the CLV3 protein in *Arabidopsis* (Nishihama et al., 2003; Lenhard and Laux, 2003). Sytemin and phytosulfokine are examples of peptide ligands derived from larger pre-proteins (Pearce

et al., 1991; Matsubayashi and Sakagami, 1996). The question that then remains to be answered is whether CLE proteins are indeed processed further into even smaller peptides, and if so, which peptide fragments are the functional ones.

Acknowledgements

References

Aloni, R., 1987. Differentation of vascular tissues. Annu. Rev. Plant Physiol. 38, 179–204.

Ausubel, F.M., Brent, R., Kingston, R.E., Moore, D.D., Seidman, J.G., Smith, J.A., Struhl, K., 1990. Current Protocols in Molecular Biology. Wiley, New York.

Benjamins, R., Quint, A., Weijers, D., Hooykaas, P., Offringa, R., 2001. The PINOID protein kinase regulates organ development in Arabidopsis by enhancing polar auxin transport. Development 128, 4057–4067.

Boutilier, K., Offringa, R., Sharma, V.K., Kieft, H., Ouellet, T., Zhang, L., Hattori, J., Liu, C.M., Van Lammeren, A.A., Miki, B.L., Custers, J.B., Van Lookeren Campagne, M.M., 2002. Ectopic expression of BABY BOOM triggers a conversion from vegetative to embryonic growth. Plant Cell 14, 1737–1749.

Brand, U., Fletcher, J.C., Hobe, M., Meyerowitz, E.M., Simon, R., 2000. Dependence of stem cell fate in Arabidopsis on a feedback loop regulated by CLV3 activity. Science 289, 617–619.

Casamitjana-Martinez, E., Hofhuis, H.F., Xu, J., Liu, C.M., Heidstra, R., Scheres, B., 2003. Root-specific CLE19 over-expression and the sol1 and sol2 suppressors implicate a CLV-like pathway in the control of Arabidopsis root meristem maintainance. Curr. Biol. 13, 1435–1441.

Christensen, S.K., Dagenais, N., Chory, J., Weigel, D., 2000. Regulation of auxin response by the protein kinase PINOID. Cell 100, 469–478.

Clough, S.J., Bent, A.F., 1998. Floral dip: a simplified method for Agrobacterium-mediated transformation of Arabidopsis thaliana. Plant J. 16, 735–743.

Cock, J.M., McCormick, S., 2001. A large family of genes that share homology with CLAVATA3. Plant Physiol. 126, 939–942.

Custers, J.M.B., Cordewener, J.H.G., Nollen, Y., Dons, H.J.M., van Lookeren Campagne, M.M., 1994. Temperature controls both gametophytic and sporophytic development in microspore cultures of Brassica napus. Plant Cell Rep. 13, 267–271.

Custers, J.B.M., Cordewener, J.H.G., Fiers, M.A., Maassen, B.T.H., van Lookeren Campagne, M.M., Liu, C.M., 2001. Androgenesis in Brassica: a model system to study the initiation of plant embryogenesis. In:

Bhojwani, S.S., Soh, W.Y. (Eds.), Current Trends in the Embryology of Angiosperm. Kluwer, London, pp. 451–470.

Datla, S.S.R., Bekkaoui, F., Hammerlindl, J.K., Pilate, G., Dunstan, D.I., Crosby, W.L., 1993. Improved high-level constitutive foreign gene expression in plants using an AMV RNA4 untranslated leader sequence. Plant Sci. 94, 139–149.

Fletcher, J.C., Brand, U., Running, M.P., Simon, R., Meyerowitz, E.M., 1999. Signaling of cell fate decisions by CLAVATA3 in Arabidopsis shoot meristems. Science 283, 1911–1914.

Groß-Hardt, R., Laux, T., 2003. Stem cell regulation in the shoot meristem. J. Cell. Sci. 116, 1659–1666.

Heck, G.R., Perry, S.E., Nichols, K.W., Fernandez, D.E., 1995. AGL15, a MADS domain protein expressed in developing embryos. Plant Cell 7, 1271–1282.

Hobe, M., Muller, R., Grunewald, M., Brand, U., Simon, R., 2003. Loss of CLE40, a protein functionally equivalent to the stem cell restricting signal CLV3, enhances root waving in Arabidopsis. Dev. Genes Evol. 213, 371–381.

Jefferson, R.A., Kavanagh, T.A., Bevan, M.W., 1987. GUS fusions: p-Glucuronidase as a sensitive and versatile gene fusion marker in higher plants. EMBO J. 6, 3901–3907.

Jürgens, G., Torres, R.A., Berleth, T., 1994. Embryogenic pattern formation in flowering plants. Annu. Rev. Genet. 28, 251–371.

Lenhard, M., Laux, T., 2003. Stem cell homeostasis in the Arabidopsis shoot meristem is regulated by intercellular movement of CLAVATA3 and its sequestration by CLAVATA1. Development 130, 3163–3173.

Li, Z., Thomas, T.L., 1998. PEI1, an embryo-specific zinc finger protein gene required for heart-stage embryo formation in Arabidopsis. Plant Cell 10, 383–398.

Liu, C.M., Meinke, D.W., 1998. The titan mutants of Arabidopsis are disrupted in mitosis and cell cycle control during seed development. Plant J. 16, 21–31.

Long, J.A., Barton, M.K., 1998. The development of apical embryonic pattern in Arabidopsis. Development 125, 3027–3035.

Matsubayashi, Y., Sakagami, Y., 1996. Phytosulfokine, sulfated peptides that induce the proliferation of single mesophyll cells of Asparagus officinalis L. Proc. Natl. Acad. Sci. U. S. A. 93, 7623–7627.

Nishihama, R., Jeong, S., DeYoung, B., Clark, S.E., 2003. Retraction. Science 300, 1370.

Olsen, A.N., Skriver, K., 2003. Ligand mimicry? Plant-parasitic nematode polypeptide with similarity to CLAVATA3. Trends Plant Sci. 8, 55–57.

Opsahl-Ferstad, H.G., Le Deunff, E., Dumas, C., Rogowsky, P.M., 1997. ZmEsr, a novel endosperm-specific gene expressed in a restricted region around the maize embryo. Plant J. 12, 235–246.

Otsuga, D., DeGuzman, B., Prigge, M.J., Drews, G.N., Clark, S.E., 2001. REVOLUTA regulates meristem initiation at lateral positions. Plant J. 25, 223–236.

Pearce, G., Strydom, D., Johnson, S., Ryan, C.A., 1991. A polypeptide from tomato leaves induces wound-inducible inhibitor protein. Science 253, 895–898.

Rojo, E., Sharma, V.K., Kovaleva, V., Raikhel, N.V., Fletcher, J.C., 2002. CLV3 is localized to the extracellular space, where it activates the Arabidopsis CLAVATA stem cell signaling pathway. Plant Cell 14, 969–977.

Sabatini, S., Beis, D., Wolkenfelt, H., Murfett, J., Guilfoyle, T., Malamy, J., Benfey, P., Leyser, O., Bechtold, N., Weisbeek, P., Scheres, B., 1999. An auxin-dependent distal organizer of pattern and polarity in the Arabidopsis root. Cell 99, 463–472.

Schoof, H., Lenhard, M., Haecker, A., Mayer, K.F., Jürgens, G., Laux, T., 2000. The stem cell population of Arabidopsis shoot meristems is maintained by a regulatory loop between the CLAVATA and WUSCHEL genes. Cell 100, 635–644.

Sessions, R.A., Zambryski, P.C., 1995. Arabidopsis gynoecium structure in the wild type and in ettin mutants. Development 121, 1519–1532.

Sharma, V.K., Fletcher, J.C., 2002. Maintenance of shoot and floral meristem cell proliferation and fate. Plant Physiol. 129, 33–39.

Sharma, V.K., Ramirez, J., Fletcher, J.C., 2003. The Arabidopsis CLV3-like

(CLE) genes are expressed in diverse tissues and encode secreted proteins. Plant Mol. Biol. 51, 415–425.

Siegfried, K.R., Eshed, Y., Baum, S.F., Otsuga, D., Drews, G.N., Bowman, J.L., 1999. Members of the *YABBY* gene family specify abaxial cell fate in *Arabidopsis*. Development 126, 4117–4128.

Smyth, D.R., Bowman, J.L., Meyerowitz, E.M., 1990. Early flower development in *Arabidopsis*. Plant Cell 2, 755–767.

van Engelen, F.A., Molthoff, J.W., Conner, A.J., Nap, J.P., Pereira, A., Stiekema, W.J., 1995. *PBINPLUS*, an improved plant transformation vector based on *pBIN19*. Transgenic Res. 4, 288–290.

Vroemen, C.W., Mordhorst, A.P., Albrecht, C., Kwaaitaal, M.A., De Vries, S.C., 2003. The *CUP-SHAPED COTYLEDON3* gene is required for boundary and shoot meristem formation in *Arabidopsis*. Plant Cell 15, 1563–1577.